

Quark production and momentum isotropization in the QGP thermalization

Sergio Barrera Cabodevila

in collaboration with

Xiaojian Du, Carlos A. Salgado and Bin Wu

based on

Phys. Lett. B 871 (2025). SBC et al. & [arXiv:2604.XXXXX]

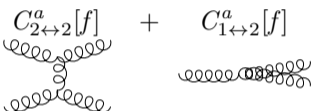


UNIVERSITÄT
HEIDELBERG
ZUKUNFT
SEIT 1386

- 1 Introduction to BEDA and comparison with EKT
- 2 Bottom-up thermalization with quarks
- 3 Azimuthal isotropization

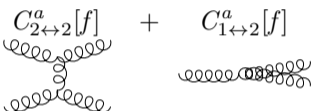
- 1 Introduction to BEDA and comparison with EKT
- 2 Bottom-up thermalization with quarks
- 3 Azimuthal isotropization

- The QCD Boltzmann equation at leading order

$$\left(\partial_t + \underbrace{\frac{\mathbf{p}}{p} \cdot \nabla_{\mathbf{x}}}_{\text{Expansion}} \right) f^a(\mathbf{x}; \mathbf{p}; t) = C_{2 \leftrightarrow 2}^a[f] + C_{1 \leftrightarrow 2}^a[f], \quad a = \{g, q, \bar{q}\}$$


The diagram for $C_{2 \leftrightarrow 2}^a$ shows two incoming wavy lines merging into two outgoing wavy lines. The diagram for $C_{1 \leftrightarrow 2}^a$ shows one incoming wavy line merging into two outgoing wavy lines.

- The QCD Boltzmann equation at leading order

$$\left(\partial_t + \underbrace{\frac{\mathbf{p}}{p} \cdot \nabla_{\mathbf{x}}}_{\text{Expansion}} \right) f^a(\mathbf{x}; \mathbf{p}; t) = C_{2 \leftrightarrow 2}^a[f] + C_{1 \leftrightarrow 2}^a[f] \quad , \quad a = \{g, q, \bar{q}\}$$


The diagram for $C_{2 \leftrightarrow 2}^a$ shows two incoming wavy lines merging into two outgoing wavy lines. The diagram for $C_{1 \leftrightarrow 2}^a$ shows one incoming wavy line merging into two outgoing wavy lines.

- Longitudinal-boost invariant expansion + infinite transverse size

$$\left(\partial_\tau - \frac{p_z}{\tau} \partial_{p_z} \right) f^a = C_{2 \leftrightarrow 2}^a[f] + C_{1 \leftrightarrow 2}^a[f] \quad , \quad a = \{g, q, \bar{q}\}$$

- Macroscopic quantities evolving during the thermalization process

$$\hat{q} = \hat{q}[f] \quad m_D^2 = m_D^2[f] \quad T_* = \frac{\hat{q}}{\alpha_s N_c \mathcal{L} m_D^2}$$

- In the weak-coupling limit \rightarrow Bottom-up thermalization
- Effective Kinetic Theory (EKT) has been widely used in this context

Phys. Lett. B 502 (2001). Baier et al.

JHEP 01 (2003). Arnold, Moore, and Yaffe

Phys. Rev. Lett. 115.18 (2015). Kurkela and Zhu

Phys. Rev. Lett. 127.12 (2021). Du and Schlichting

- Boltzmann Equation in Diffusion Approximation (BEDA) keeps most of the relevant physics.

JHEP 06 (2024). SBC, Salgado, and Wu

Phys. Lett. B 871 (2025). SBC et al.

	BEDA	EKT
$C_{2\leftrightarrow 2}$	Only small angle scatterings \Rightarrow Fokker-Planck + source term	Full $2 \leftrightarrow 2$ QCD dynamics @LO
$C_{1\leftrightarrow 2}$	Deep LPM regime	Both LPM and Bethe-Heitler

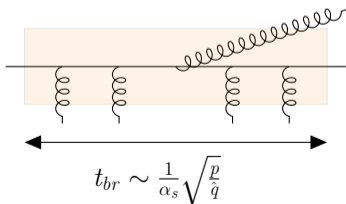
$$\hat{q}_a = 8\pi\alpha_s^2 C_a \log \frac{\langle p_t^2 \rangle}{m_D^2} \int \frac{d^3 p}{(2\pi)^3} \left[N_c f(1+f) + \frac{N_f}{2} F(1-F) + \frac{N_f}{2} \bar{F}(1-\bar{F}) \right]$$

- Shows up when integrating the IR divergencies

Nucl. Phys. B 572 (2000). Mueller

- m_D^2 is given by BEDA, but $\langle p_t^2 \rangle$ needs to be estimated by the broadening:

$$\langle p_t^2 \rangle \sim \hat{q} \tau_{char} \sim \hat{q} t_{br}$$



$$\log \frac{\langle p_t^2 \rangle}{m_D^2} = \log \left(\frac{\sqrt{\hat{q} p}}{\alpha_s m_D^2} \right) + \mathcal{O}(\log \log) \xrightarrow[\text{equilibrium}]{\text{thermal}} \log \frac{1}{\alpha_s} \checkmark$$

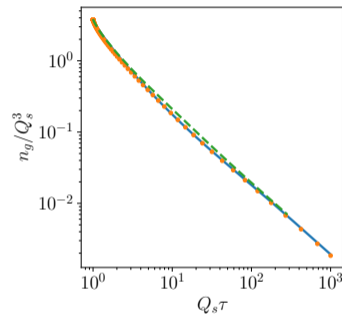
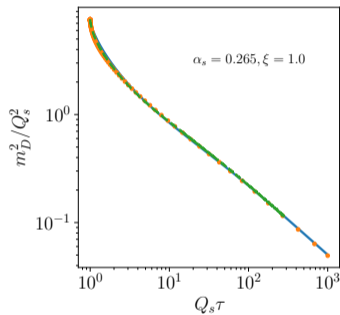
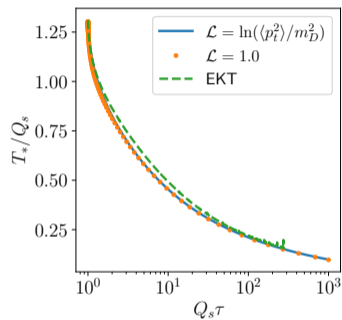
- Evolve from CGC-like initial conditions

Phys. Rev. Lett. 115.18 (2015). Kurkela and Zhu

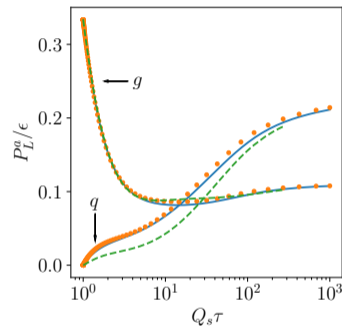
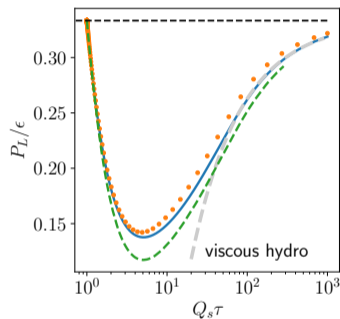
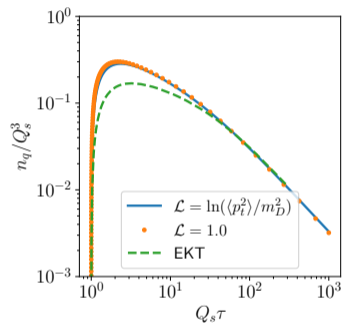
Phys. Rev. D 99.5 (2019). Kurkela and Mazeliauskas

$$f_0 = \frac{A}{4\pi N_c \alpha_s} \frac{e^{-\frac{2}{3}((p_z \xi)^2 + p_\perp^2)/Q_0^2}}{\sqrt{((p_z \xi)^2 + p_\perp^2)/Q_0^2}}, \quad F_0 = 0,$$

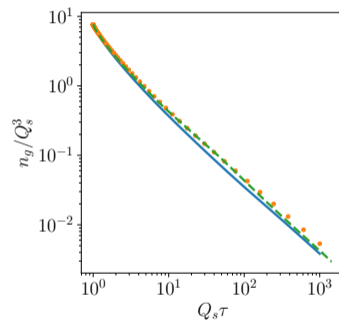
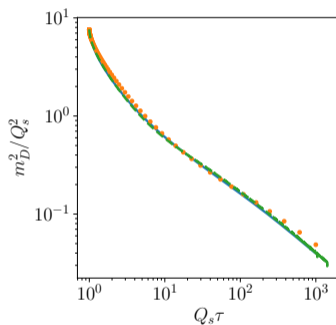
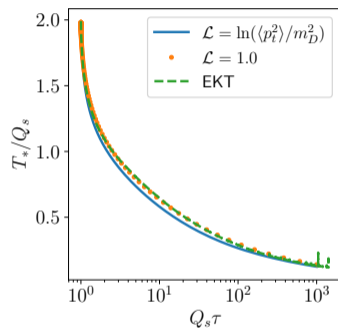
- $\xi \rightarrow$ Quantifies anisotropy (taken as 0 for this comparison)
- $Q_0, A \rightarrow$ Phenomenological parameters fitting CGC
- Initial time $\tau_0 = Q_s^{-1}$



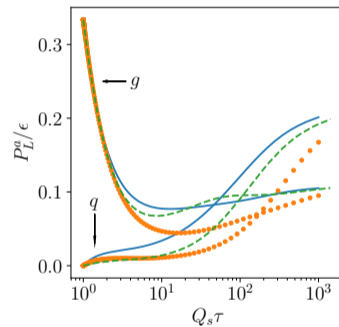
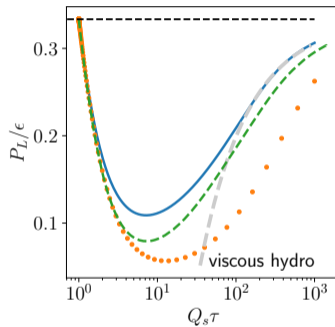
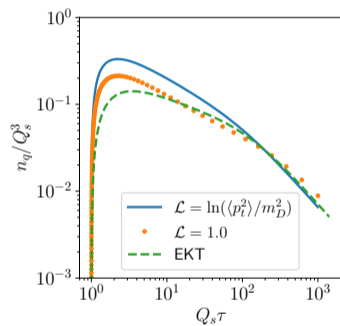
- Nice quantitative agreement during whole evolution
- Gluon number density dominated by expansion



- Quantitative differences in n_q due to differences in $g \rightarrow q\bar{q}$ splitting rates
- Higher n_q systematically leads to higher P_L/ϵ



- Still nice quantitative agreement



- The time dependent logarithm improves the accord with EKT

- 1 Introduction to BEDA and comparison with EKT
- 2 Bottom-up thermalization with quarks
- 3 Azimuthal isotropization

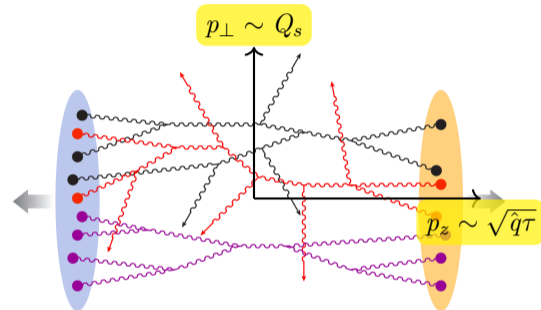
- Assume Bjorken expansion

Phys. Rev. D 27 (1983). Bjorken

- Partons propagating along z -direction quickly fly away from the system

→ Typical momentum given by broadening $p \sim \sqrt{\hat{q}\tau} \Rightarrow$ **Soft partons**

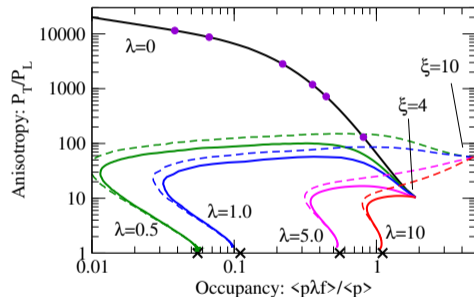
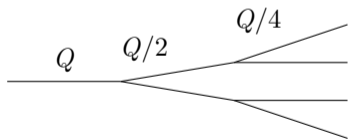
- Partons moving along the transverse plane remain in the system with $p \sim Q_s \Rightarrow$ **Hard partons**



- There are three different stages for thermalization when considering boost-invariant expansion

Phys. Lett. B 502 (2001). Baier et al.

- 1 System dominated by expansion
- 2 Collision and expansion contribute similarly
- 3 Democratic cascade speeds up the thermalization



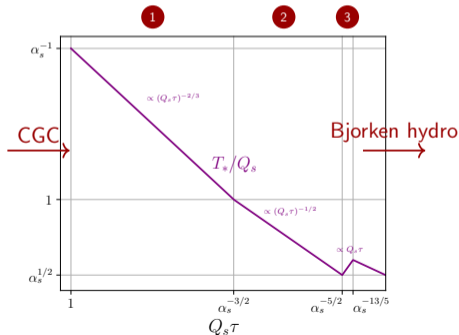
Phys. Rev. Lett. 115.18 (2015). Kurkela and Zhu

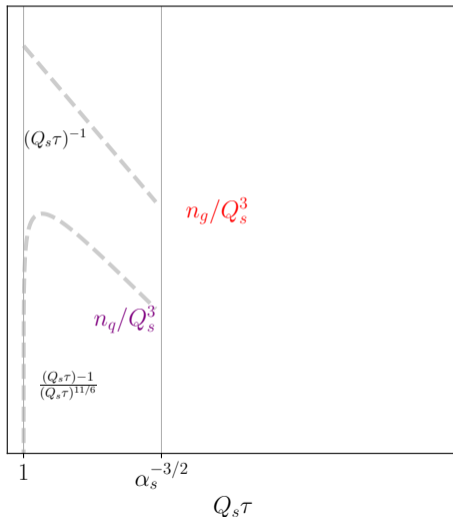
- Assume a parametrically highly populated and isotropic

$$f_0 \sim \frac{1}{\alpha_s}, \quad F = 0$$

- Parametric behaviour is well known for the pure gluon scenario

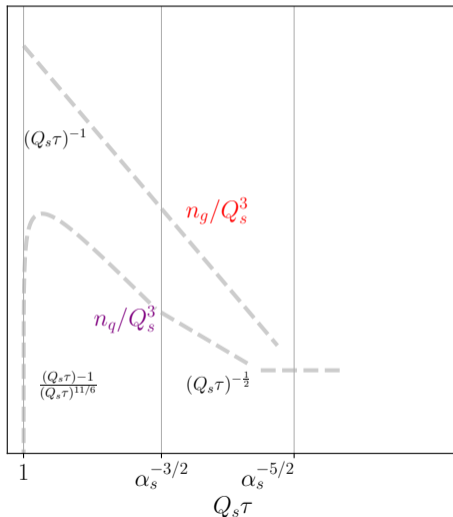
Phys. Lett. B 502 (2001). Baier et al.





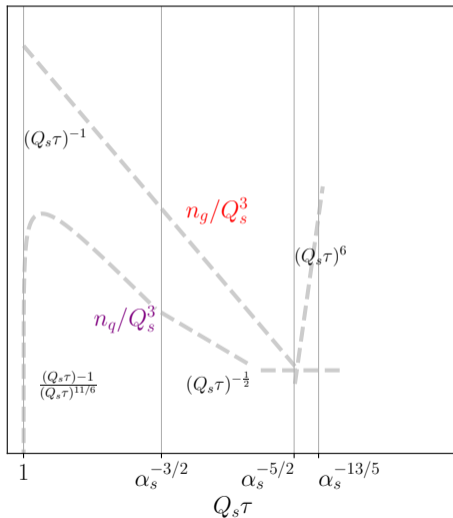
First stage $1 \ll Q_s\tau \ll \alpha_s^{-3/2}$

- Gluon number density dominated by hard gluons decreases due to expansion
- Quark number density is dominated by $g \rightarrow q\bar{q}$ splitting
- Rapidly reaches its peak and then decreases with the expansion



Second stage $\alpha_s^{-3/2} \ll Q_s \tau \ll \alpha_s^{-5/2}$

- Most gluons are still hard \rightarrow expansion dominated
- Change in \hat{q} changes the scaling in quark production
- At $Q_s \tau \sim \alpha_s^{-2}$ quark production starts to be dominated by soft gluons via $g \rightarrow q\bar{q}$ and $gg \rightarrow q\bar{q}$ and keeps n_q constant

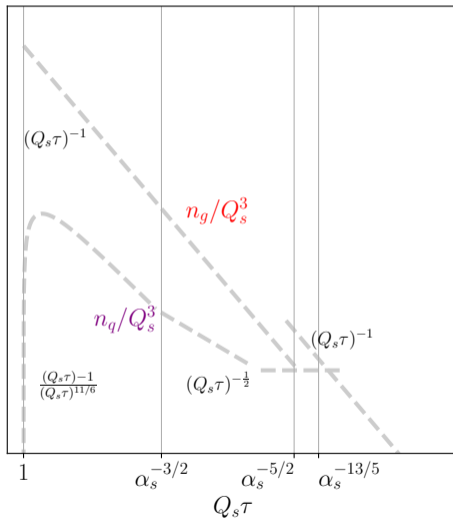


Third stage $\alpha_s^{-5/2} \ll Q_s \tau \ll \alpha_s^{-13/5}$

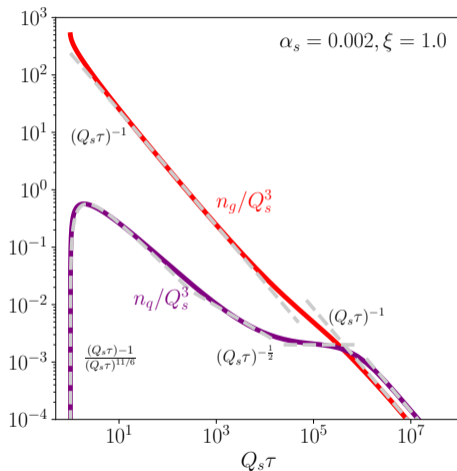
- Most partons are thermal

$$n_g \sim n_q \sim T^3$$

- Remaining hard partons reheat the QGP

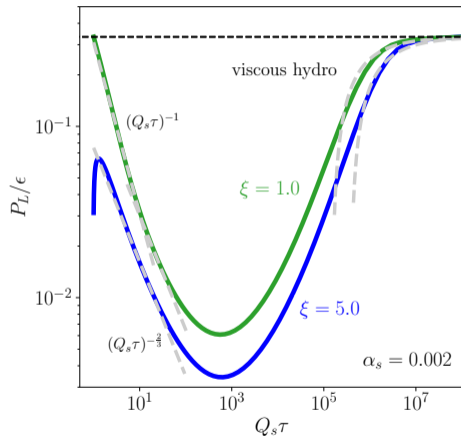


Bjorken hydro $\alpha_s^{-13/5} \ll Q_s\tau$

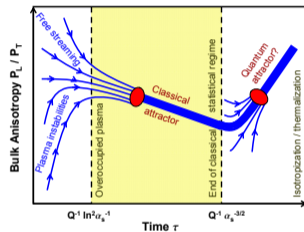


Comparison with numerics

- Nice agreement with numerical simulations
- Reheating stage missing since α_s is not small enough



- System quickly converges to non-thermal fixed point scaling at early times

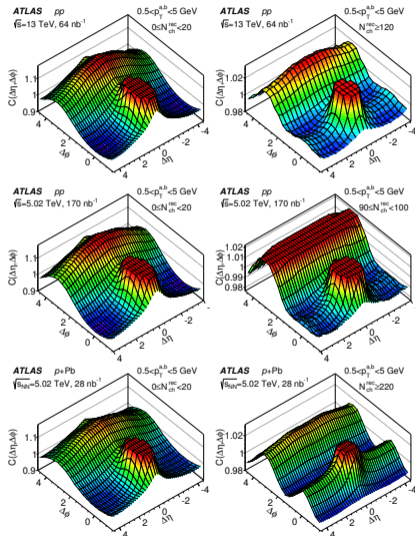


Phys. Rev. D 89.7 (2014). Berges et al.

- At later times, system approaches to viscous hydro

$$\frac{P_L}{\epsilon} = \frac{1}{3} - \frac{16}{9} \frac{\eta}{s} \frac{1}{T_{hydro} \tau}$$

- 1 Introduction to BEDA and comparison with EKT
- 2 Bottom-up thermalization with quarks
- 3 Azimuthal isotropization**

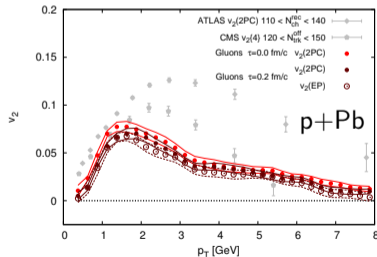


- Similar ridge to that in heavy-ion collision has been observed in small systems

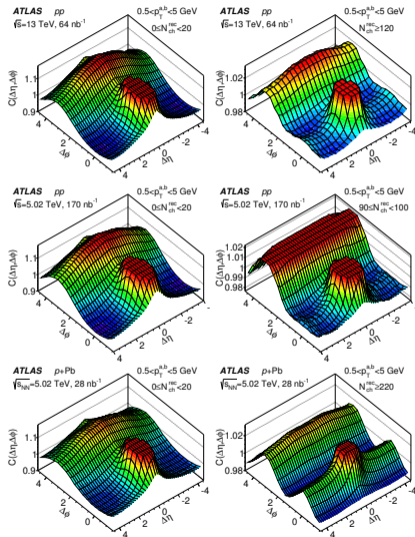
Phys. Rev. C 96.2 (2017). Aaboud et al.

- Hydrodynamics might not be the cause
- Initial state mechanisms have been proposed to explain it.

Eur. Phys. J. A 56.8 (2020). Altinluk and Armesto



Phys. Lett. B 747 (2015). Schenke, Schlichting, and Venugopalan



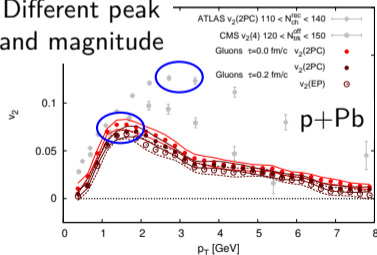
- Similar ridge to that in heavy-ion collision has been observed in small systems

Phys. Rev. C 96.2 (2017). Aaboud et al.

- Hydrodynamics might not be the cause
- Initial state mechanisms have been proposed to explain it.

Eur. Phys. J. A 56.8 (2020). Altinoluk and Armesto

Different peak and magnitude



Phys. Lett. B 747 (2015). Schenke, Schlichting, and Venugopalan

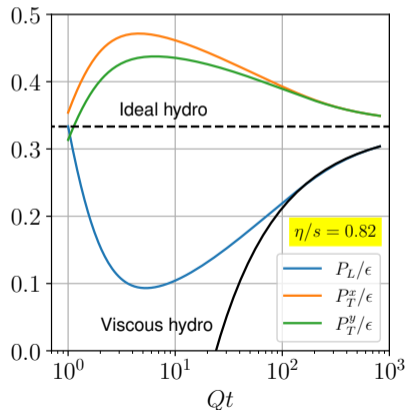
$$\frac{d^6 N}{d^3 \mathbf{x} d^3 \mathbf{p}} \sim f(\mathbf{x}; \mathbf{p}; t_f) \Rightarrow \frac{d^3 N}{d^3 \mathbf{p}} \sim \int d^3 \mathbf{x} f(\mathbf{x}; \mathbf{p}; t_f) = f(\mathbf{p}; t_f)$$

- We study how initial anisotropies relax in Kinetic Theory
- Initial condition

$$f_0(\mathbf{p}) = f_0(\mathbf{p}_T) \left(1 + \sum_n v_n^0(\mathbf{p}_T) \cos(n\phi) \right)$$

- Harmonic coefficients computed in the Event Plane

$$v_n(\mathbf{p}_T; t) = \frac{\int d\phi \cos(n(\phi - \psi_n)) f(\mathbf{p}; t)}{\int d\phi f(\mathbf{p}; t)}$$



- Start initializing with constant anisotropy and explore fully integrated v_n

$$v_n^0(\mathbf{p}_T) = v_n^0 \quad v_n(t) \equiv \frac{\int d^3\mathbf{p} \cos(n(\phi - \psi_n)) f(\mathbf{p}; t)}{\int d^3\mathbf{p} f(\mathbf{p}; t)}$$

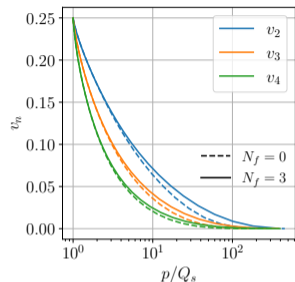
- Exploring the variation due to the $C_{2 \leftrightarrow 2}$ kernel

$$\begin{aligned} \partial_\tau v_n(\tau) = & \frac{\hat{q}}{4n_g} \int \frac{dp}{(2\pi)^2} \frac{d(\cos \theta)}{p^2} \left[- \frac{n^2 v_n^2 \tilde{f}/2}{p^2(1 - \cos^2 \theta)} \right. \\ & + \frac{1}{T_*} \left(\frac{2\tilde{f}}{p} + \partial_p \tilde{f} \right) v_n^2 \\ & \left. + \frac{1}{T_*} \left(\frac{2\tilde{f}^2}{p} + \partial_p \tilde{f}^2 \right) \left(v_n^2 + \sum_{k,l} v_k v_l \int \frac{d\phi}{2\pi} \cos(n\phi) \cos(k\phi) \cos(l\phi) \right) \right] \end{aligned}$$

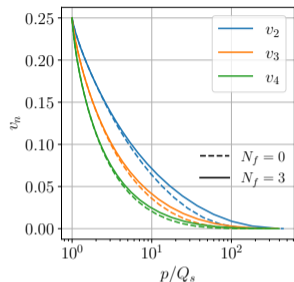
Higher n relaxes faster

Produces higher n anisotropies

- For initial v_n , only v_{kn} with $k = 1, 2, 3 \dots$ are produced

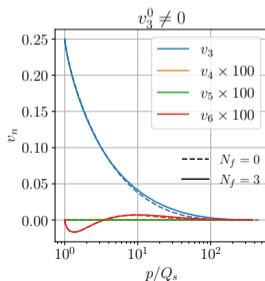
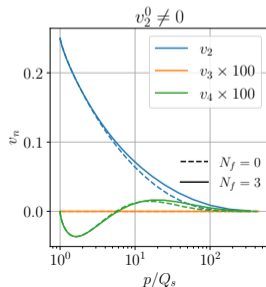


- Higher n relaxes faster
- Including quarks in the system delays the isotropization



- Higher n relaxes faster
- Including quarks in the system delays the isotropization

- For initial v_n , only v_{kn} with $k = 1, 2, 3 \dots$ are produced

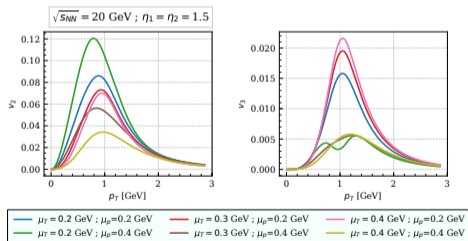
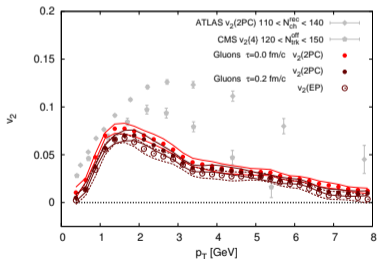


- Based on different results from initial state interactions we model

Eur. Phys. J. A 56.8 (2020). Altinoluk and Armesto

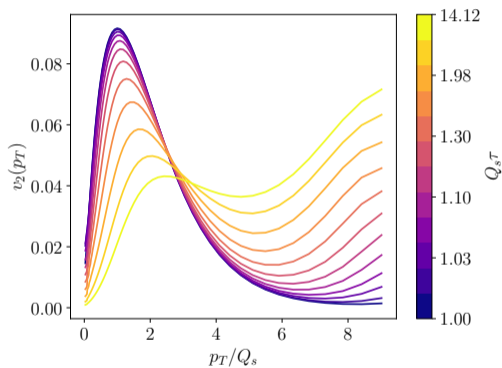
$$f_0(\mathbf{p}) = f_0(\mathbf{p}_T) \left(1 + \sum_n v_n^0(\mathbf{p}_T) \cos(n\phi) \right), \quad v_n^0(p_T) = \tilde{v}_n \frac{p}{Q} e^{-|p|/Q}$$

- In the following results we take $v_2 = 0.25$ and $v_{n \neq 2} = 0$



Phys. Lett. B 747 (2015). Schenke, Schlichting, and Venugopalan

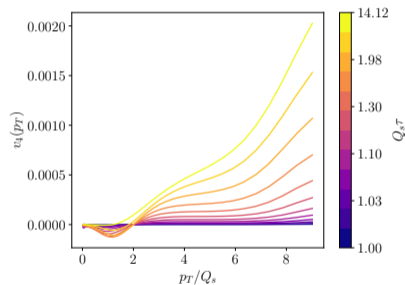
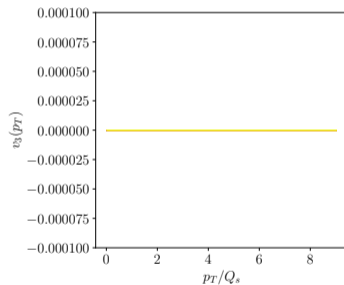
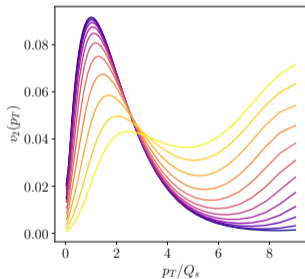
Eur. Phys. J. C 79.9 (2019). Agostini, Altinoluk, and Armesto

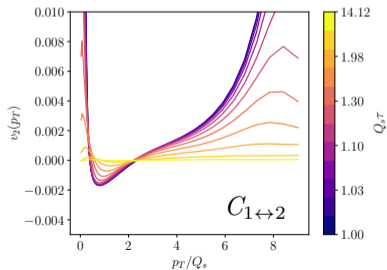
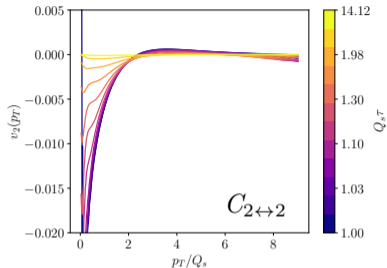


$$v_n(p_T; t) = \frac{\int dp_z d\phi \cos(n(\phi - \psi_n)) f(\mathbf{p}; t)}{\int d\phi f(\mathbf{p}; t)}$$

- The magnitude of the anisotropy decreases with time
- The position of the maximum is shifted to higher momenta
- Anisotropy at large p_T is produced easily because of the low occupancy in this region

- Initial $v_2 \Rightarrow$ only even harmonics are generated





● Infrared:

- $C_{1\leftrightarrow 2} \rightarrow$ Increases v_2 due to **collinear radiation** of partons from the more anisotropic regions of the phase space
- $C_{2\leftrightarrow 2} \rightarrow$ Decreases the anisotropy more efficiently than $C_{1\leftrightarrow 2}$

● Ultraviolet:

- $C_{1\leftrightarrow 2} \rightarrow$ Increases v_2 due to **collinear merging** of partons in the more anisotropy regions of the phase space
- $C_{2\leftrightarrow 2} \rightarrow$ Modifies v_2 less efficiently

- Same initial condition as before

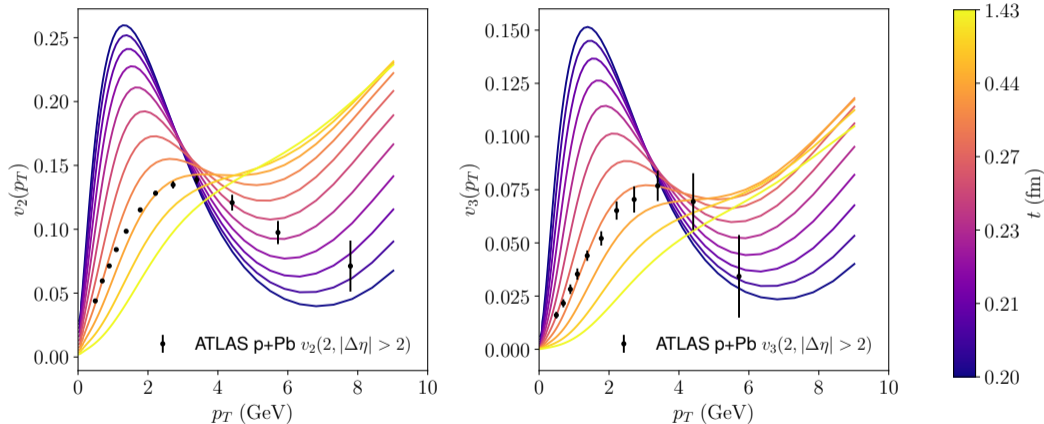
$$f_0(\mathbf{p}) = f_0(\mathbf{p}_T) \left(1 + \sum_n v_n^0(\mathbf{p}_T) \cos(n\phi) \right), \quad v_n^0(p_T) = \tilde{v}_n \frac{p}{Q} e^{-|p|/Q}$$

- Parametrization to reproduce energy density from $p + Pb$ collisions at LHC

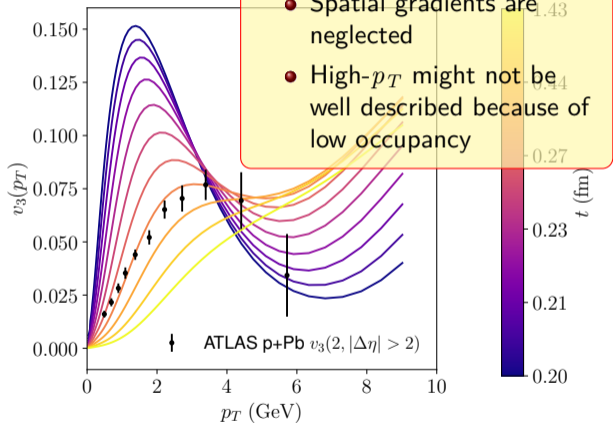
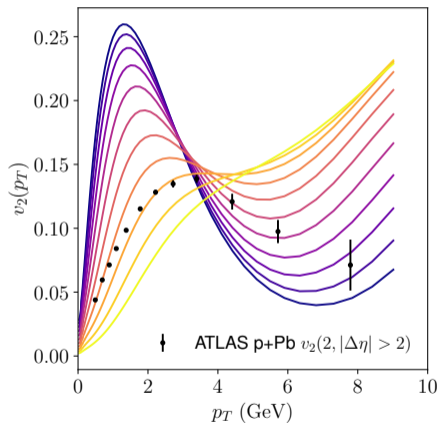
JHEP 11 (2021). Kurkela, Mazeliauskas, and Törnkvist

- Initial time for the kinetic stage set to $t_0 = 0.2$ fm
- Initialize anisotropy with $\tilde{v}_2 = 0.75$, $\tilde{v}_3 = 0.45$ and $\tilde{v}_{n \neq 2,3} = 0$
- Position of the maximum set to $Q \sim Q_s \approx 1.22$ GeV

- Experimental data can be mimicked at a time $t \sim 0.5$ fm



- Experimental data can be mimicked at a time $t \sim 0.5$ fm



Disclaimer

- Spatial gradients are neglected
- High- p_T might not be well described because of low occupancy

- We have shown that BEDA is qualitatively consistent with EKT
- Quark production has been parametrically understood in the bottom-up picture
- Both non-thermal fixed point and hydrodynamical attractor show up in the simulations
- Study of azimuthal isotropization in the BEDA framework indicate that final state interactions may be relevant if initial momentum anisotropies are present
- Final state interactions introduce a mechanism which shifts the maximum of the azimuthal anisotropy to higher p_T , as experimental data suggests
- Include spatial gradients will allow to perform a more complete study of the collective behavior of the bulk

- We have shown that BEDA is qualitatively consistent with EKT
- Quark production has been parametrically understood in the bottom-up picture
- Both non-thermal fixed point and hydrodynamical attractor show up in the simulations
- Study of azimuthal isotropization in the BEDA framework indicate that final state interactions may be relevant if initial momentum anisotropies are present
- Final state interactions introduce a mechanism which shifts the maximum of the azimuthal anisotropy to higher p_T , as experimental data suggests
- Include spatial gradients will allow to perform a more complete study of the collective behavior of the bulk

Thank you for your attention!

Back-up

- In diffusion approximation, the $2 \leftrightarrow 2$ collision kernel can be expressed as a Fokker-Planck equation plus an additional source term.

Phys. Lett. B 475 (2000). Mueller

Nucl. Phys. A 930 (2014). Blaizot, Wu, and Yan

$$C_{2 \leftrightarrow 2}^a = \frac{1}{4} \hat{q}_a(t) \nabla_p \cdot \left[\nabla_p f^a + \frac{\mathbf{v}}{T^*(t)} f^a (1 + \epsilon_a f^a) \right] + \mathcal{S}_a$$

$$\mathcal{S}_q = \frac{2\pi\alpha_s^2 C_F^2 \ln \frac{\langle p_t^2 \rangle}{m_D^2}}{p} \left[\mathcal{I}_c f (1 - F) - \bar{\mathcal{I}}_c F (1 + f) \right],$$

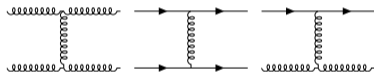
$$\mathcal{S}_{\bar{q}} = \mathcal{S}_q|_{F \leftrightarrow \bar{F}}, \quad \mathcal{S}_g = -\frac{N_f}{2C_F} (\mathcal{S}_q + \mathcal{S}_{\bar{q}}),$$

- In diffusion approximation, the $2 \leftrightarrow 2$ collision kernel can be expressed as a Fokker-Planck equation plus an additional source term.

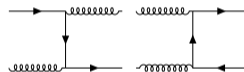
Phys. Lett. B 475 (2000). Mueller

Nucl. Phys. A 930 (2014). Blaizot, Wu, and Yan

Fokker-Planck term



Source term



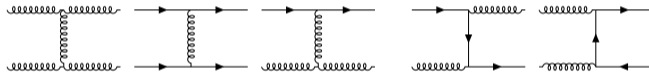
- In diffusion approximation, the $2 \leftrightarrow 2$ collision kernel can be expressed as a Fokker-Planck equation plus an additional source term.

Phys. Lett. B 475 (2000). Mueller

Nucl. Phys. A 930 (2014). Blaizot, Wu, and Yan

Fokker-Planck term

Source term



- The gluon distribution function is known to diverge at small p , $f \propto 1/p$, for over-occupied systems, which is interpreted as the onset of Bose-Einstein Condensation (BEC).

Nucl. Phys. A 920 (2013). Blaizot, Liao, and McLerran

- The presence of BEC can be studied numerically by choosing the appropriate boundary conditions with¹ $\dot{n}_c \propto (\lim_{p \rightarrow 0} pf - T_*)$.

Nucl. Phys. A 930 (2014). Blaizot, Wu, and Yan

¹ $n_c \equiv$ number density of the BEC.

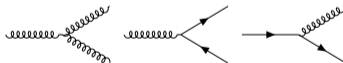
- The $1 \leftrightarrow 2$ kernel can be computed in the deep LPM regime

Nucl. Phys. B 483 (1997). Baier et al.

Phys. Rev. D 78 (2008). Arnold and Dogan

$$C_{1 \leftrightarrow 2}^a = \int_0^1 \frac{dx}{x^3} \sum_{b,c} \left[\frac{\nu_c}{\nu_a} C_{ab}^c(p/x; p, p(1-x)/x) - \frac{1}{2} C_{bc}^a(p; xp, (1-x)p) \right]$$

- The $C_{bc}^a(p; xp, (1-x)p)$ describes the collinear splitting $a \leftrightarrow bc$.
- The three possible processes involved are the three QCD interaction vertices.



- Will the BEC still appear in initially over-populated system after including inelastic collisions?

- At small p , the $g \leftrightarrow gg$ and $g \leftrightarrow q\bar{q}$ are the dominant processes in the production of gluons and (anti)quarks, respectively.
- The distributions of gluons and quarks quickly fill a thermal distribution up to small soft momentum p_s

$$f^g(p) \approx \frac{T_*}{p} \quad \text{for } p \lesssim p_g$$

$$f^q(p) \approx \frac{1}{e^{-\frac{\mu_*}{T_*}} + 1} \quad \text{for } p \lesssim p_q$$

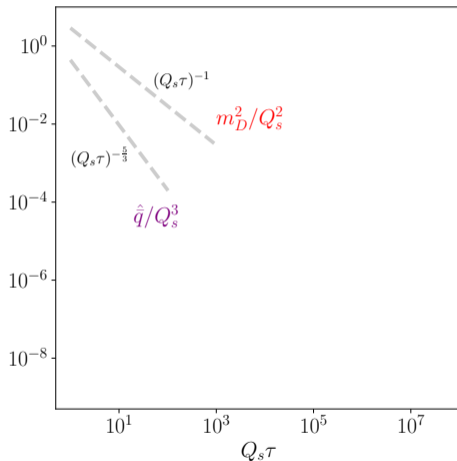
At early times, p_s is given by ($\mathcal{I}_c = \mathcal{I}_c[f]$)

$$p_g \equiv (\hat{q}_A m_D^4 t^2 / 2)^{\frac{1}{5}} \quad p_q \equiv [\alpha_s C_F \pi (\mathcal{I}_c + \bar{\mathcal{I}}_c) t]^{\frac{2}{5}} \hat{q}_F^{\frac{1}{5}}$$

- This behavior implies that $\dot{n}_c = 0$, so no BEC is observed as in the pure gluon case.

Nucl. Phys. A 961 (2017). Blaizot, Liao, and Mehtar-Tani

JHEP 06 (2024). SBC, Salgado, and Wu



First stage $1 \ll Q_s \tau \ll \alpha_s^{-3/2}$

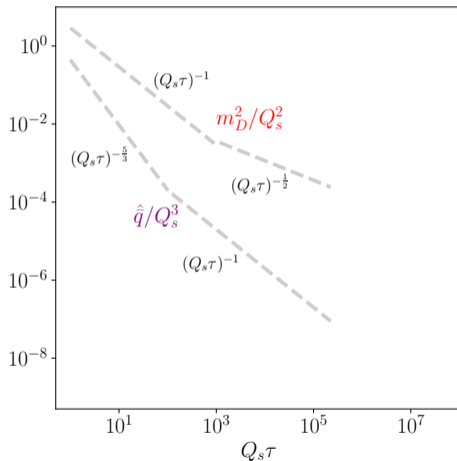
- Most partons in the system are hard and dominated by the expansion

$$n_g \sim \frac{1}{\alpha_s} \frac{Q_s^3}{Q_s \tau}, \quad f_g \gg 1$$

- Screening and \hat{q} dominated by hard gluons

$$m_D^2 \sim \alpha_s \frac{n_g}{Q_s} \sim \frac{Q_s^2}{Q_s \tau}$$

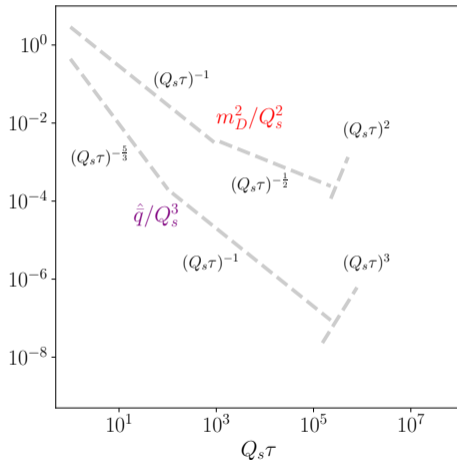
$$\hat{q} \sim \alpha_s^2 n_g f_g$$



Second stage $\alpha_s^{-3/2} \ll Q_s \tau \ll \alpha_s^{-5/2}$

- Most of gluons are still hard but $f_g \ll 1$
- Screening is dominated by soft gluons
- \hat{q} changes scaling due to Bose enhancement

$$\hat{q} \sim \alpha_s^2 n_g (1 + f)$$

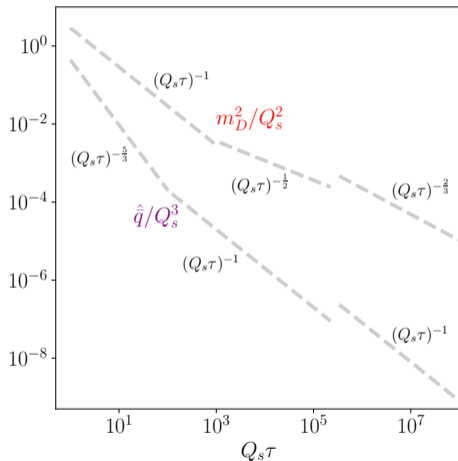


Third stage $\alpha_s^{-5/2} \ll Q_s \tau \ll \alpha_s^{-13/5}$

- Most partons in the system are soft and in thermal equilibrium

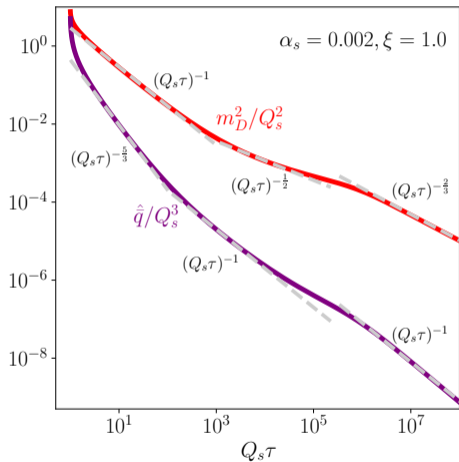
$$n_g \sim T^3 \quad m_D^2 \sim \alpha_s T^2 \quad \hat{q} \sim \alpha_s^2 T^3$$

- Remaining soft partons cascade and reheat the soft bath



Bjorken hydro $\alpha_s^{-13/5} \ll Q_s \tau$

- Full system has thermalized and evolves as in Bjorken hydro



Comparison with numerics